In-situ residual strength prediction of carbon-fiber composites using machine learning

B. Kamouni[1,2*], A. Ebrahimi[1,2], F. Shadmehri[1,2]

[1] Concordia Center for Composites (CONCOM), Department of Mechanical, Industrial and Aerospace Engineering, Concordia University, Montreal, Canada

[2] Research Center for High Performance Polymer and Composite Systems (CREPEC), Montreal, Canada

* *Corresponding author (badr-eddine.kamouni@mail.concordia.ca)*

Keywords: *Structural health monitoring; fatigue loading; residual strength prediction; machine learning; carbon nanotube*

1. Abstract

An approach for in-situ residual strength prediction was investigated for carbon/epoxy composite samples subjected to fatigue loading by using a piezoresistivity-based structural health monitoring method with machine learning. This study evaluates the feasibility of using piezoresistivity in conductive carbon/epoxy rectangular coupons to extract meaningful electrical resistance (ER) data for residual strength prediction through machine learning techniques. In this process, a conductive epoxy matrix was first obtained by incorporating carbon nanotubes (CNTs). The fatigue tests, which were performed on the samples to introduce various levels of damage, were monitored by ER measurements periodically collected from two distinct gauge areas using a 4-probe method. Afterwards, quasi-static tensile tests until failure were performed on the samples to evaluate their residual strengths. The ER features most strongly related to residual strength were identified and used as inputs for several machine learning algorithms, including Ridge regression, K-Nearest Neighbors (KNN), Decision Tree (DT), Random Forest (RF), Extreme Gradient Boosting (XGBoost), and Support Vector Regression (SVR). In addition, a stacking ensemble approach was implemented by combining the predictions of the standalone models. Despite the limited dataset size, the analysis demonstrated the predictive potential of this data-driven approach. The best-performing model in this study was a DT meta-model that integrated the predictions of all standalone models as input features, achieving a cross-validation mean absolute percentage error (MAPE) of 4.41% for residual strength prediction on the training/validation dataset.

2. Introduction

Composite materials, especially carbon fiber-reinforced polymers (CFRPs), are utilized in a wide range of applications due to their high specific strength and stiffness compared to conventional metals [1]. A relevant challenge in structural integrity analysis of CFRPs is the accurate prediction of how damage progresses in the material. Structural health monitoring (SHM) methods are commonly used to estimate critical prognostics, such as residual strength and remaining service life. By detecting and analyzing damage-related signals in-situ, these approaches provide insight into the current condition of a component [2-4]. However, the complexity of damage mechanisms, including interface debonding, fiber rupture, matrix cracking and delamination, makes data interpretation challenging, time-consuming, and potentially inaccurate when using traditional physical models. In response to these challenges, data-driven approaches based on machine learning have been increasingly used in SHM to enable more efficient predictions of structural health from complex monitoring signals [4-6].

A recent study demonstrated that piezoresistivity-based approaches combined with machine learning can accurately predict the residual strength of glass/epoxy composites enhanced with carbon nanotubes (CNTs), which provide electrical conductivity [4]. This work explores the feasibility of applying a similar approach to carbon/epoxy composites subjected to fatigue loading, where the inherent conductivity of carbon fibers poses additional challenges compared to insulating glass fibers. The objective is to assess whether electrical resistance (ER) measurements are sufficiently sensitive and relevant for SHM of carbon/epoxy systems.

Several studies have applied piezoresistive approaches to CFRPs under fatigue loading to relate ER change to several mechanisms of damage accumulation. For that material system, fiber cracking is generally associated with an irreversible ER increase since that damage mechanism directly breaks the electrically conductive paths through the laminate [7-11]. However, matrix cracking is the more common form of damage that occurs before fiber fracture and represents most of the accumulated damage [9,11]. This type of damage is correlated with an increase in electrical resistance in non-conductive fiber composites with matrices impregnated with CNTs that make them conductive [4]. However, cracks in these conductive matrices have a limited effect on the electrical response when dominated by conductive carbon fibers. Instead, the added conductivity provided by CNTs is shown, for example, to result in smoother electrical readings [10]. The complexity of analyzing ER change in carbon/epoxy laminates also arises from the mechanisms that cause the ER to decrease during fatigue. The literature provides several potential explanations for this decrease. In carbon composites made from woven fabrics, the electrical resistivity is mainly governed by the fiber-to-fiber contacts in both the transverse and through-thickness directions, which are affected by the level of fiber waviness [7]. The irreversible change in fiber arrangement during cyclic loading can create enhanced electrically conductive networks in the composite, thus contributing to some stochastic decrease in ER [8,10]. Another potential explanation is related to matrix cracking which promotes fiber-to-fiber contacts and enhances the conductive network through the material [9-11]. Therefore, for CFRPs, the complex ER patterns that develop throughout fatigue loading motivate the use of data-driven machine learning approaches for residual strength prediction.

3. Experimental Procedure

3.1. Materials and sample manufacturing

Carbon 2×2 twill-weave fabrics ($205\ g/m^2$) purchased from Texonic were used as reinforcement. Hexion Epon 862 and Epikure Curing Agent W were used, respectively, as the epoxy resin and curing agent for the matrix system. Single-walled carbon nanotubes (SWCNTs) with a purity of 75 % and an aspect ratio of $10^3 - 10^4$, obtained from TUBALL, were used to make the matrix electrically conductive. Silver epoxy adhesive, procured from AI Technology Inc, was used to create electrical contacts for the probes.

To manufacture the samples, the first stage involved dispersing CNTs into the epoxy resin. Following the related study [4], the resin was mixed with a suitable amount of SWCNTs, which was selected to be 0.1 wt.% relative to the resin weight. A uniform mixture was made using a three-roll mill (EXAKT 80E) as shown in Figure 1-a. This resin mixture was then combined with the Epikure curing agent at 26.4 wt.% relative to the resin weight, as specified by its datasheet. A vacuum mixer (THINKY ARV-200) was used to minimize air entrapment in the final CNT/epoxy mixture. The second stage included the hand layup process to make the composite laminate (Figure 1-b). The epoxy mixture was applied to 4 layers of carbon fiber fabrics before the placement of standard ancillary materials. The layup assembly was then vacuum-bagged and cured in an autoclave for one dwell of 2 hours at 25 psi and 350 °F (Figure 1-c). The third stage consisted of bonding the glass-epoxy tabs to the laminate plates, which were then cut into coupons with a width of 15.00 ± 0.15 mm. Two tabs, each 4 cm in length, were therefore bonded on both ends of composite coupons 23 cm long. The design and dimensions of the samples were made according to ASTM D3039/D3039M-17 when applicable. Adhesive templates were then attached to each sample for repeatable probe attachment. This helped implement the 4-probe method for 2 gauge lengths of 59.5 mm. Probes were installed over each slit on the template and covered with silver epoxy adhesive before being cured for 8 hours at 80 ℃ (Figure 1-d). A subset of the final labelled samples is shown in Figure 1-e.

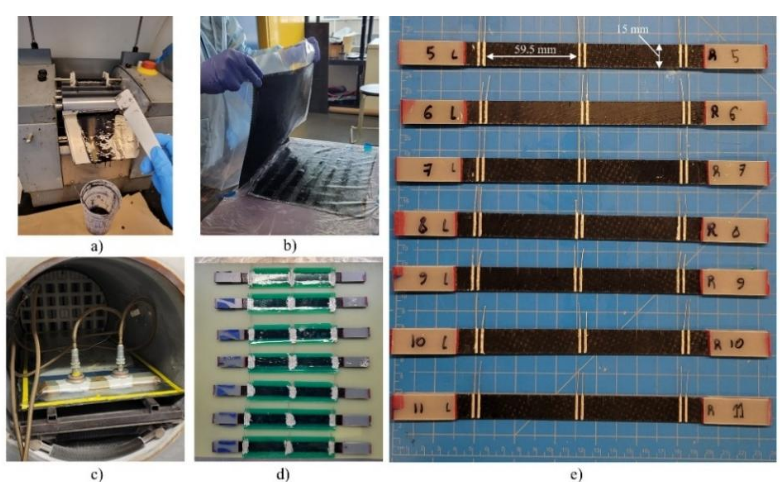

Figure 1. Manufacturing process for the composite coupons: a) CNT dispersion in epoxy using a three-roll mill, b) hand layup process, c) autoclave curing, d) probe attachment using the template, e) final labelled samples

3.2. Testing apparatus

The same 4-probe method described in [4] was applied to minimize variations in probe contact resistance due to fatigue-induced damage. As shown in Figure 2, this method is implemented with 2 gauge areas where a constant 1 milliampere (I) was applied on the outer probes while the voltage (V) was measured on the inner probes. Since the center probes were shared, these measurements were done sequentially. The ER was then computed using Ohm's law. The objective of having 2 gauge areas was to provide a level of damage localization within the ER data. This was done by allowing the predictive capability of each gauge to be evaluated separately during model training.

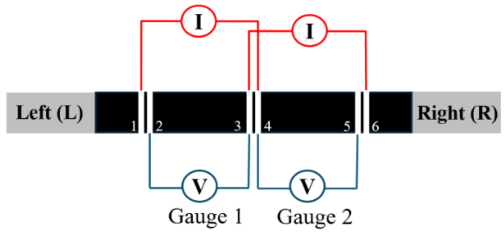

Figure 2. Schematic of the 4-probe method applied on 2 distinct gauge areas of a sample

The constant current was applied using a current source (Keithley 6220 DC) and the voltage was measured using a nanovoltmeter (Keithley 2182A). A switch system (Keithley 7001) was used to allow sequential ER measurement at both gauge areas. The quasi-static and fatigue tests were performed using a 100 kN universal testing machine (MTS Model 318). Figure 3 shows the main testing apparatus used for this study.

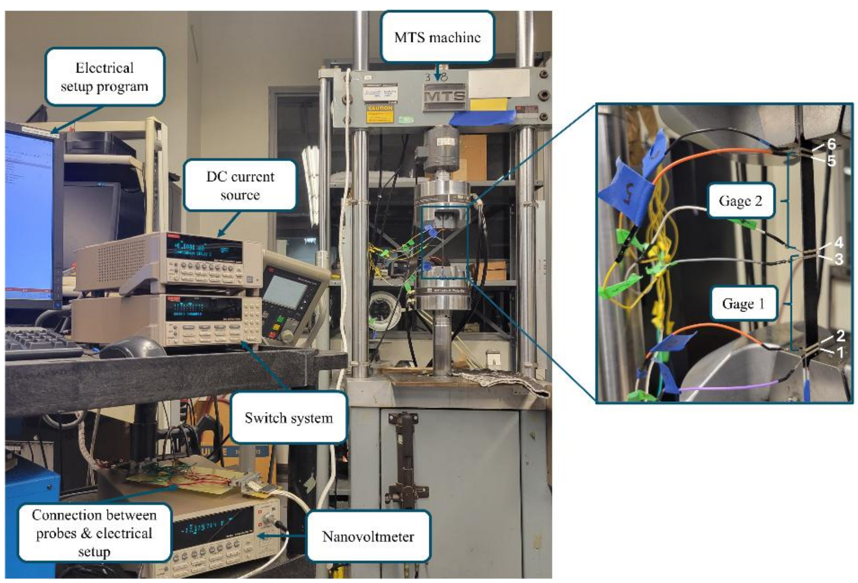

Figure 3. Testing apparatus used to take ER measurements during fatigue loading

3.3. Fatigue test

Before starting the main experiments, the tensile strength of the material was estimated from an average of 5 samples subjected to a quasi-static tensile test until failure. The tensile strength was found to be $1007 \pm 30\ MPa$. A series of experiments was conducted on 21 samples. The samples were first subjected to a tension-tension cyclic loading to induce damage to the material. The fatigue tests were conducted at a frequency of 2 Hz with a minimum load ratio of 0.1 (load applied / material strength). For this study, a maximum load ratio of 0.7 was applied to most of the samples. To evaluate model performance on unseen samples, 4 samples were set aside as the test set, so only 17 samples were used for training/validation. Two of these test set samples were subjected to a different load ratio of 0.8, which was not included in the training/validation set, to provide an initial assessment of model robustness under a new loading scenario. To create different levels of damage, the samples were subjected to 4000, 6000, 8000 or 10000 cycles at those loading conditions. At 200-cycle intervals, the fatigue test was momentarily stopped and held at the maximum load ratio to extract the ER measurements at both gauges. Following a similar procedure as in [4], ER measurements at 20% increments of the fatigue test ($ER_{20\%}, ER_{40\%}, ER_{60\%}, ER_{80\%}$ & $ER_{100\%}$) were used to build the input features for the algorithms. Additionally, the ER before loading (ER_i) and at the peak of loading before the first fatigue cycles ($ER_{0\%}$) were also extracted for each sample. After the fatigue test, the samples were subjected to a quasi-static tensile loading until failure to find their residual strengths. A summary of the experiments for all 21 samples, which includes the training/validation and test split for the machine learning algorithms, the fatigue loading conditions and the residual strengths for each sample, is provided in Table 1. Note that sample IDs 7, 12 and 13 were not included since they failed prematurely during their fatigue tests.

Table 1. Summary of the experiment

Sample Set	Sample ID	Number of Cycles	Residual Strength (MPa)	Maximum Load Ratio
Training/Validation	2	10000	831	0.7
	4	10000	1023	0.7
	5	10000	956	0.7
	6	8000	982	0.7
	8	6000	891	0.7
	9	10000	730	0.7
	10	6000	912	0.7
	11	6000	960	0.7
	16	8000	935	0.7
	17	8000	1054	0.7
	18	8000	994	0.7
	19	8000	779	0.7
	20	6000	1045	0.7
	21	4000	976	0.7
	22	4000	879	0.7
	23	4000	1080	0.7
	24	4000	822	0.7
Test	1	8000	818	0.7
	3	10000	779	0.7
	14	4000	934	0.8
	15	4000	996	0.8

4. Residual Strength Prediction Method

4.1. Initial feature pool

From the ER measurement data extracted during the fatigue tests, the main objective was to identify potential features most strongly related to residual strength. Similar approaches used in the related study [4] were considered: the total ER change (ΔER_T) and the relative ER change (ΔER_R). The total ER change considers the entire resistance variation between an ER measured during fatigue loading at any 20% increment (ER_f) and the initial measurement without any load (ER_i). This can be calculated as an absolute (1) or percentage (2) total change.

$$\Delta ER_T(abs) = ER_f - ER_i \tag{1}$$

$$\Delta ER_T(\%) = \left(\frac{ER_f - ER_i}{ER_i}\right) \times 100 \tag{2}$$

Five features were built using the above formulas in absolute and percentage variations: $\Delta ER_{T,20\%}$, $\Delta ER_{T,40\%}$, $\Delta ER_{T,60\%}$, $\Delta ER_{T,80\%}$ and $\Delta ER_{T,100\%}$. The relative ER change represents the variation in electrical response between consecutive measurement points. ER_f denotes the current measurement and ER_{f-1} the previous measurement obtained 20% of the total number of cycles earlier. This can also be calculated as an absolute (3) or percentage (4) relative change.

$$\Delta ER_R(abs) = ER_f - ER_{f-1} \tag{3}$$

$$\Delta ER_R(\%) = \left(\frac{ER_f - ER_{f-1}}{ER_i}\right) \times 100 \tag{4}$$

Five features were extracted using the relative approach in absolute and percentage variations: $\Delta ER_{R,0\%-20\%}$, $\Delta ER_{R,20\%-40\%}$, $\Delta ER_{R,40\%-60\%}$, $\Delta ER_{R,60\%-80\%}$ and $\Delta ER_{R,80\%-100\%}$. In addition, ER_i and the difference between the initial ER and the ER at the maximum loading ratio before starting the fatigue test ($ER_{0\%} - ER_i$) were considered as 2 additional features, for a total of 12 features considered. Figure 4 depicts the obtained experimental results for 2 of the features using the absolute formulas applied on gauge 1 ER data. Since there is variation between feature datasets in their absolute or percentage form, both gauge areas were subdivided into absolute and percentage feature datasets accordingly. Therefore, each algorithm was separately trained on 4 different datasets (labelled as % gauge 1, % gauge 2, ABS gauge 1 and ABS gauge 2).

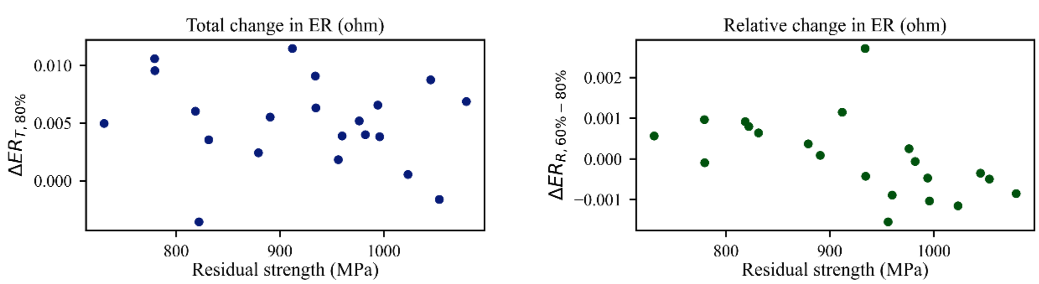

Figure 4. Total and relative ER change features in their absolute variation for gauge 1

4.2. Feature selection

From the initial feature pool, a forward feature selection (FFS) method [4] was used to find the optimal feature set for each model. This method progressively adds one feature at a time, starting from an empty feature set, while monitoring the overall prediction performance of the model. At each step, the candidate feature that provides the best improvement in model performance is selected. The process continues until the addition of further features no longer improves the model performance or leads to a decrease in prediction quality.

4.3. Machine learning algorithms

Several machine learning algorithms, known to perform well with small datasets [4], were used to predict residual strength from ER data in CNT-impregnated carbon/epoxy composite samples. The algorithms considered were Ridge regression, Support Vector Regression (SVR), K-Nearest Neighbor (KNN), Decision Tree (DT), Random Forest (RF) and Extreme Gradient Boosting (XGBoost). They were implemented as standalone prediction models and within a stacking ensemble learning approach. As shown in Figure 5, this approach uses preliminary predictions of residual strengths from the base models to create a new dataset. A meta-model, which uses any of the 6 standalone algorithms, is trained on those first-level predictions to establish a refined relationship between the ER data and the actual residual strengths. All models, whether standalone or in a stacking ensemble, were trained on standardized data.

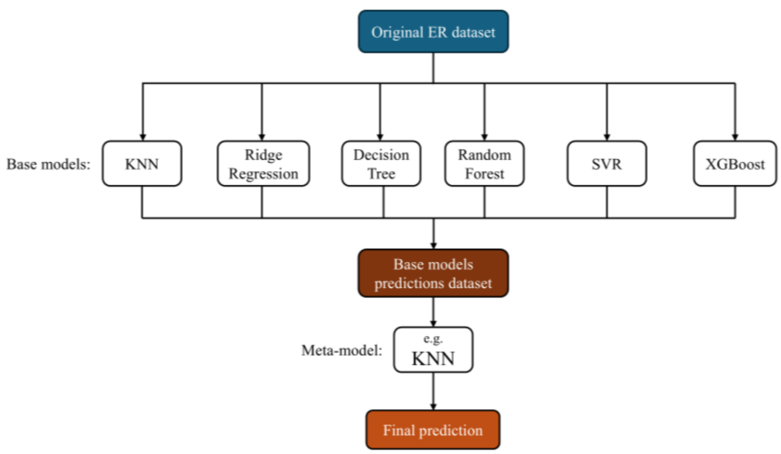

Figure 5. Structure of the stacking ensemble approach

The training and optimization process for each model was performed using a two-step iterative process in which FFS was coupled with hyperparameter optimization. Before training, a predefined range of hyperparameters was established for each model. At each feature-selection step, the model was trained iteratively on this restricted dataset to carry out a hyperparameter grid search optimization. Each training sub-step used 5-fold cross-validation. This process was repeated until a hyperparameter-tuned model was obtained with a feature set that no longer improved model performance. The performance metric used was the following mean absolute percentage error (MAPE) formula:

$$\text{MAPE}\ (\%) = \frac{1}{n}\sum_{i=1}^{n}\left|\frac{y_i - \hat{y}_i}{y_i}\right| \times 100 \tag{5}$$

where n is the number of data points in the validation set, y_i is the actual residual strength of the i^{th} sample within that validation set and $\hat{y}_i$ is the predicted residual strength for this sample.

5. Results and Discussion

As mentioned previously, each model was trained on 4 different types of datasets that separate gauge 1 and 2 ER measurements in their absolute or percentage feature form. Table 2 shows the results of the FFS applied on the standalone models using the feature dataset from gauge 1 in its absolute variation.

Table 2. Optimal feature set for each standalone model following forward feature selection (using ABS gauge 1 dataset)

Sequence	Models					
	Ridge	KNN	SVR	DT	RF	XGBoost
1	$\Delta ER_{R,60\%-80\%}$	$\Delta ER_{R,60\%-80\%}$	$\Delta ER_{R,60\%-80\%}$	$\Delta ER_{R,60\%-80\%}$	$\Delta ER_{R,60\%-80\%}$	$\Delta ER_{R,60\%-80\%}$
2	$ER_{0\%} - ER_i$	-	$ER_{0\%} - ER_i$	$\Delta ER_{T,20\%}$	$\Delta ER_{R,0\%-20\%}$	$\Delta ER_{T,20\%}$
3	-	-	-	$\Delta ER_{R,20\%-40\%}$	-	$\Delta ER_{R,0\%-20\%}$
4	-	-	-	$\Delta ER_{R,0\%-20\%}$	-	-
5	-	-	-	-	-	-
6	-	-	-	-	-	-

The FFS results can highlight important features based on how frequently they are selected across different models. Frequent selection would show that these features may be strongly related to the residual strength of this material system. For this experiment, the 3 most relevant features, in order of frequency of occurrence, were found to be $\Delta ER_{R,60\%-80\%}$, $(ER_{0\%} - ER_i)$ and $\Delta ER_{R,0\%-20\%}$. This suggests that, for the present carbon/epoxy system, relative ER changes are more relevant for prediction because they provide better insight into incremental ER variations compared to total ER change. Since the literature shows that, for CFRPs, there exist damage mechanisms that cause ER to increase or decrease [7-11], a feature that accumulates the ER response throughout the fatigue test might be less useful for predicting residual strengths due to the competing ER changes when damage accumulates. Figure 6 shows the performance of standalone models and meta-models based on their average cross-validation MAPE obtained for each training/validation dataset type. For standalone models, gauge 1 data produced slightly better predictions in general except for RF. Also, absolute features yielded predictions that were approximately equal to, or slightly better than, those obtained using percentage-based features. Tree-based models (DT, RF and XGBoost) generally outperformed the regression-based models (Ridge, SVR) and the distance-based model (KNN). The best standalone model was a DT trained using gauge 1 data in either absolute or percentage variation, reaching a MAPE of 5.69%. Also depicted in Figure 6 are the meta-models' performances. The ensemble learning approach did not consistently improve prediction performance across all dataset types. This is reflected by the weaker cross-validation performance of Ridge and SVR as parent models and by the fact that the trends observed across dataset types for the standalone models were not reproduced for the meta-models. However, an improved prediction was still possible in one case, with a DT meta-model using preliminary predictions based on the % gauge 2 dataset achieving the lowest average cross-validation MAPE of 4.41%. Figure 7 shows the absolute percentage error (APE), corresponding to Eq. (5) with $n = 1$, on the unseen test set for the best standalone models and the best DT meta-model. The DT meta-model reached a maximum APE of 10.60%, which was observed for sample ID 14. Overall, these results suggest that using meta-models can reduce the variability of prediction errors by combining information from base models.

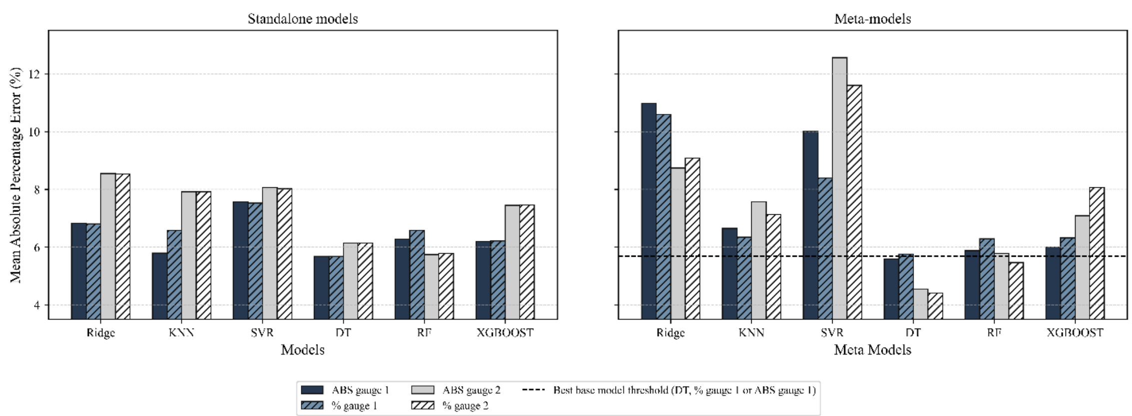

Figure 6. Average cross-validation MAPE of standalone models and meta-models for each training/validation dataset type

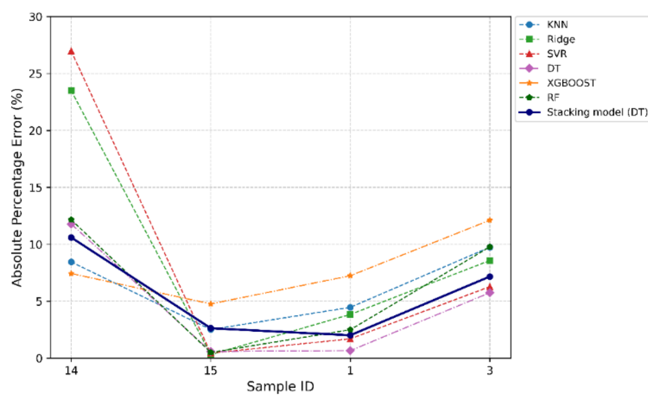

Figure 7. Absolute percentage error in prediction of the best standalone models and meta-model on the test set

6. Conclusion

A procedure was developed to predict the residual strength of CNT-impregnated carbon/epoxy composites subjected to fatigue loading. This was achieved using a piezoresistivity-based SHM approach combined with machine learning algorithms as prediction tools. ER measurements were periodically extracted from the samples during fatigue testing and converted into suitable input features for the machine learning models. Using a forward feature selection algorithm coupled with a hyperparameter grid search, each model was trained and optimized using 17 samples and tested on 4 unseen samples. Future work should consider a larger sample pool to improve prediction generalization. Additional investigations could also be conducted on carbon/epoxy samples without CNTs to analyze differences in the extracted ER data and the resulting predictions.

7. References

[1] J. Zhang, G. Lin, U. Vaidya, and H. Wang. "Past, present and future prospective of global carbon fibre composite developments and applications". *Composites Part B: Engineering*, Vol. 250, Art. No. 110463, 2023, doi: 10.1016/j.compositesb.2022.110463.

[2] S. Hassani, M. Mousavi, and A. H. Gandomi. "Structural Health Monitoring in Composite Structures: A Comprehensive Review". *Sensors*, Vol. 22, Art. No. 153, 2021, doi: 10.3390/s22010153.

[3] Y. Zhang et al. "Advances in sensors technologies for composites structural health monitoring". *Composite Structures*, Vol. 370, Art. No. 119448, 2025, doi: 10.1016/j.compstruct.2025.119448.

[4] A. Ebrahimi, F. Shadmehri, and S. Van Hoa. "In-situ residual strength prediction of composites subjected to fatigue loading". *Composites Part A: Applied Science and Manufacturing*, Vol. 187, Art. No. 108490, 2024, doi: 10.1016/j.compositesa.2024.108490.

[5] X. Qing et al. "Machine Learning Based Quantitative Damage Monitoring of Composite Structure". *International Journal of Smart and Nano Materials*, Vol. 13, No. 2, pp 167–202, 2022, doi: 10.1080/19475411.2022.2054878.

[6] G. Scarselli and F. Nicassio. "Machine Learning for Structural Health Monitoring of Aerospace Structures: A Review". *Sensors*, Vol. 25, Art. No. 6136, 2025, doi: 10.3390/s25196136.

[7] Y. Tao et al. "A comprehensive review on fiber-based self-sensing polymer composites for in situ structural health monitoring". *Advanced Composites and Hybrid Materials,* Vol. 8, Art. No. 339, 2025, doi: 10.1007/s42114-025-01413-y.

[8] X. Wang, S. Wang, and D. D. L. Chung. "Sensing damage in carbon fiber and its polymer-matrix and carbon-matrix composites by electrical resistance measurement". *Journal of Materials Science,* Vol. 34, pp 2703–2713, 1999.

[9] V. Kostopoulos, A. Vavouliotis, P. Karapappas, P. Tsotra, and A. Paipetis. "Damage Monitoring of Carbon Fiber Reinforced Laminates Using Resistance Measurements. Improving Sensitivity Using Carbon Nanotube Doped Epoxy Matrix System". *Journal of Intelligent Material Systems and Structures*, Vol. 20, No. 9, pp 1025–1034, 2009, doi: 10.1177/1045389X08099993.

[10] A. Vavouliotis, A. Paipetis, and V. Kostopoulos. "On the fatigue life prediction of CFRP laminates using the Electrical Resistance Change method". *Composites Science and Technology*, Vol. 71, No. 5, pp 630–642, 2011, doi: 10.1016/j.compscitech.2011.01.003.

[11] X. Wang and D. D. L. Chung. "Mechanical damage in carbon fiber polymer-matrix composite, studied by electrical resistance measurement". *Composite Interfaces*, Vol. 9, No. 1, pp 51–60, 2002.